HHS Public Access

Author manuscript

Proteomics. Author manuscript; available in PMC 2015 June 26.

Published in final edited form as:

Proteomics. 2008 July ; 8(13): 2750–2763. doi:10.1002/pmic.200700986.

Differential Proteomics in the Aging Noble Rat Ventral Prostate

Ying Wai Lam[1,3], **Neville N.C. Tam**[1,3], **James E. Evans**[2], **Karin M. Green**[2], **Xiang Zhang**[1,3], and **Shuk-mei Ho**[1,3,4]

[1]Department of Environmental Health, Division of Environmental Genetics and Molecular Toxicology, University of Cincinnati College of Medicine, Cincinnati, OH

[2]Department of Biochemistry and Molecular Pharmacology, University of Massachusetts Medical School, Worcester, MA

[3]Part of the work was conducted at the Department of Surgery, Division of Urology, University of Massachusetts Medical School, Worcester, MA

Abstract

Incidence of prostatic diseases increases dramatically with age which may be related to a decline in androgen support. However, the key mechanisms underlying prostate aging remain unclear. In the present study, we investigated the aging process in the ventral prostate of Noble rats by identifying differentially expressed prostate proteins between 3- and 16-month-old animals using ICAT and MS. In total, 472 proteins were identified with less than a 1% false positive rate, among which 34 were determined to have a greater than 2-fold increase or 1.7-fold decrease in expression in the aged VPs versus their younger counterparts. The majority of the differentially expressed proteins identified have not been previously reported to be associated with prostate aging, and they fall into specific functional categories, including oxidative stress/detoxification, chaperones, protein biosynthesis, vesicle transport and intracellular trafficking. The expression of glutathione S-transferase, ferritin, clusterin, kininogen, oxygen regulated protein 150, spermidine synthase, ADP ribosylation factor and cyclophilin B was verified by Western blot analyses on samples used for the ICAT study, as well as on those obtained from an independent group of animals comprised of three age groups. To our knowledge, this is the first study on the proteome of the aging rat prostate.

Keywords

Chaperone; Isotope-coded affinity tags; Oxidative stress; Quantitative proteomics; Testosterone levels

INTRODUCTION

The incidence of prostatic diseases increases dramatically with age. An American man over 60 years old has a 1 in 7 chance of being diagnosed with prostate cancer, but only a probability of 1 in 53 between the fourth and fifth decades of life [1]. Furthermore, benign

[4]To whom correspondence should be addressed: Shuk-mei Ho, Ph.D., Department of Environmental Health, University of Cincinnati College of Medicine, Cincinnati, Ohio, 45267. Tel: 513-558-5701; Fax: 513-558-0071; shuk-mei.ho@uc.edu.

prostatic hyperplasia is detected in 70% of men in their sixties. A number of age-related changes have been implicated in the pathogenesis of prostatic diseases, including a decline in androgen support [2], accumulation of DNA damage [3], reduction in apoptotic potential [4], increase in inflammation [5–7], and oxidative stress (OS) due to loss or decreased activity of antioxidant enzymes [8–10]. Moreover, the involvement of growth and survival factors and changes in sensitivity of the aged prostate to hormones [9, 11–16] have been suggested to contribute to the hyperproliferative characteristics of prostatic diseases in elderly men, who experience a decline in androgen levels. Finally, changes in tissue microenvironment have also been suggested to be involved in the development of prostatic disorders [17–19]. Modulation of prostate epithelial cells by fibroblast senescence has been shown to occur via paracrine mechanisms [20, 21]. Despite these research findings, a comprehensive picture of prostate aging is still lacking.

Global profiling of gene expression changes has been the mainstay technology used to study the molecular mechanisms of prostate aging in animal models [8, 22, 23]. We previously performed a transcriptional profiling of ventral prostates (VPs) from Noble rats aged 3- and 16-months. This animal model was chosen because the Noble rat strain has a shorter life span of < 2 years than most other rat strains that live over 3 years [24]. We showed that changes in the expression of specific genes in the aged VPs helped explain many distinctive morphological features of aging in the gland [8]. The expression of genes related to amino acid metabolism, protein synthesis, secretion and degradation, vesicle/membrane trafficking, energy metabolism, and cellular defense against stress, was reduced in aged VPs, which display signs of wide-spread inflammatory infiltration, atrophy and/or apoptotic activities of the luminal epithelial cells, and clear evidence of reduced luminal secretory activities [8]. In contrast, expression of genes related to cell survival (TRPM2 or clusterin) was found to be elevated. Reyes et al. [22] observed similar but not identical findings, reporting that in aging ACI rat dorsolateral prostates (DLPs) genes with differential expression were mainly those associated with inflammation, OS, tissue remodeling and energy metabolism, and with the activation of growth signaling involving prolactin, interleukin 6, and hepatocyte growth factor.

In the present study, we investigate the impact of aging on the proteome of Noble rats VPs. Recent advances in proteomic technologies allow accurate identification and quantification of thousands of proteins in a complex mixture with the use of isotope labeling and mass spectrometry. The commonly adopted approach involves isotopic labeling of the proteomes to be compared, either before or after enzymatic digestion, followed by analysis of the resulting peptides by mass spectrometry techniques. This strategy presents advantages over traditional two-dimensional gel electrophoresis, including more accurate quantification and broader dynamic range [25–29]. In addition, the inclusion of a gel-based fractionation step before tryptic digestion to separate labeled proteins has been proven to be robust, with the added benefit of providing molecular weight information of the target proteins.

We have successfully applied such an approach in this study to globally identify over 400 proteins and determine that thirty-four are differentially expressed (greater than 2-fold increase or 1.7-fold decrease) in the aged VP compared with its younger counterpart. Using literature-based pathway analyses, 22 out of these 34 proteins were mapped to a network

linked to TNF-α signaling. The expression of glutathione S-transferase, ferritin, clusterin, kininogen, oxygen regulated protein 150, spermine synthase, ADP ribosylation factor and cyclophilin B was verified by Western blot analyses on samples used for the ICAT study, as well as in an independent set of samples. To our knowledge, this is the first study on the proteome of the aging prostate.

MATERIALS AND METHODS

Animals and dissection of VPs

Noble rats were purchased from Charles River Breeding Laboratory (MA) and housed in the animal facility at the University of Massachusetts Medical School. The rats were fed rat chow and water *ad libitum*. The VPs of Noble rats were dissected from 3-, 12-, and 16-month-old rats, divided into several pieces of approximately 50 mg each, immediately snap-frozen and stored at −80° C until protein extraction. All animal usage protocols were approved by the Institutional Animal Care and Usage Committee at the University of Massachusetts Medical School.

Radioimmunoassay (RIA) of serum testosterone levels

Serum total testosterone levels from animals aged 4, 5, 9 and 16 (n=3–6) months were measured by RIA, which was conducted in the ILAT Steroid RIA Laboratory, University of Massachusetts Medical School (Worcester, MA). The RIA kit for testosterone assay (Coat-A-Count Total Testosterone) was provided by Diagnostic Products (Los Angeles, CA). The sensitivity of the assay was 0.04 ng/ml. RIA was performed according to the manufacturer's instructions. Each sample was measured in duplicate.

Sample preparation for MS analysis

VPs were homogenized in 2% SDS/40 mM Tris-HCl (pH 11) using a 0.2 ml micro-glass tissue grinder. The homogenates were sonicated and heat-denatured, followed by centrifugation at 10,000 g to remove cell debris. Protein content was determined using the BCA protein assay (Pierce, IL). The samples were pooled for analysis due to the limited availability of material from the rat ventral prostate tissues. One mg of total protein from pooled young (Y, n = 4) and old (O, n = 3) animal prostate lysates was subjected to cleavable isotope-coded affinity tag (ICAT™) labeling (Applied Biosystems, CA) according to the manufacturer's protocol. Briefly, after disulfide reduction with tris-(2-carboxyethyl)phosphine, total protein (1mg) from the young and old groups was labeled with 10 vials of acid cleavable "light" and "heavy" reagents, respectively. The labeled samples were combined (2 mg in total), concentrated by vacuum centrifugation to less than 100 μl, loaded onto a 3 mm thick, 14 cm long SDS-polyacrylamide gel, and subjected to electrophoretic separation at 50 mA for 5 h (Hoefer, CA). Following electrophoresis, the gel was stained with Coomassie Brilliant Blue, de-stained and scanned with an infrared detection system (LI-COR Biosciences, NE) at 800 nm to detect the Coomassie blue-stained bands. The gel lane containing separated labeled proteins was excised into 38 gel segments (Figure 2). Each gel segment was further de-stained, dehydrated with ACN and subjected to overnight tryptic digestion with 1.25 μg trypsin (Promega, WI) in 40 mM ammonium bicarbonate. Following tryptic digestion, the supernatant was collected and peptides were

extracted twice with 200 µl 50% ACN/1% acetic acid with sonication. The extracts from each gel segment were combined (~1 ml in total) and concentrated to less than 10 µl. The labeled peptides were captured on an avidin column according to the manufacturer's protocol, followed by acid cleavage of and release of the labeled peptides. The peptides were then evaporated to dryness under vacuum centrifugation and stored at −80°C until LC-MS/MS analysis.

LC-MS

The extracted peptides were dissolved in 2% formic acid. The peptide content of each of the 38 digests was determined by CBQCA assay and roughly equal amounts of peptides in each digest (about half of the sample) were analyzed by capillary LC-MS/MS using a Finnigan LTQ linear quadrupole ion trap mass spectrometry system (Thermo Fisher Scientific, MA). The peptides were first trapped on a 300 µm i.d. × 5 mm, 5 µm, 100Å C-18 PepMap column (LC Packings, CA) with a 35 µl/min flow of 2% ACN, 0.1% formic acid. The flow was then reversed and reduced to 350 nl/min through the trapping column, and directed onto the 75 µm × 100 mm PicoFrit capillary column (New Objective, MA). The solvent system was composed of 0.1% formic acid in water (A) and 0.1% formic acid in ACN (B). The gradient was programmed as follows: 2% B for 4 min, 2–12% B in 8 min, 12–45% B in 73 min, and 45–98% B in 19 min. The LTQ was operated in data dependent Triple Play™ mode with one full survey scan (*m/z* 500–2000), followed by a ZoomScan™ and a product ion scan of the zoom-scanned ion. The product ion scans were acquired with a 2.0 unit isolation width and normalized collision energy of 35.0. Ions selected for product ion scans were placed on an exclusion list for the following 60 sec. An average of 58 cycles was performed per min.

Identification of differentially expressed proteins, protein classification, and pathway analysis

The product ion spectra were searched against a rat subset of the International Protein Index (IPI) database (v3.28, downloaded on April 20 2007, 41515 entries) using the SEQUEST search engine in Bioworks 3.3. The database containing sequences in forward and reverse orientations (target-decoy, 83030 entries) that were used to limit the false positive rate to less than 1% [30, 31] was indexed with the following: fully enzymatic activity and two missed cleavage sites allowed for trypsin; peptides MW of 500–6000 Da; and an addition of 227.13 Da on cysteine as fix modification. SEQUEST search parameters were as follow: mass tolerance of 2 and 1 amu for precursor and fragment ions, respectively; three differential/PTM allowed per peptide; variable modification on methionine (+15.99 amu for oxidized methionine) and cysteine (+9.00 amu for heavy ICAT label). Analysis was performed using Bioworks 3.3 by incorporating the search files (.srf) into multiple consensus reports. As the program allows the incorporation of only 15 srf files into a single consensus report, three reports were thus generated [report 1 (gel band No. 36, 37, 38, 1–12; MW 42.7 – 240 kD), report 2 (gel band No. 13–26; 16.1 – ~40 kDa), report 3 (gel band No. 27–35; ~5 kD –15 kD)]. After applying filters of XCorr [1.5(1+), 2.0 (2+), 2.5(3+)] and DelCN (=/> 0.1), protein identifications in each of the consensus report were ranked by protein probability P(pro). 1% FP cut-off was then determined in each of the three consensus reports and the identifications with less than 1% FP were combined in a spreadsheet. Ratios of heavy versus light isotopomers were determined by XPRESS in Bioworks 3.3 (Thermo

Fisher Scientific, MA), with a mass tolerance of 1.5, minimum threshold of 50000, and number of smooth point as 5. CV was calculated for the expression ratio of peptides in their respective proteins in the Excel spreadsheet. Proteins with a median expression ratio (O/Y) of > 2 fold and < 0.58 fold, and a CV of less than 45% were considered to be differentially expressed. However, clusterin (O/Y of 2.99 with a CV of 48.12%) was included as differentially expressed as it was previously demonstrated by our gene expression microarray analysis and subsequent real-time PCR to have an increased expression in the prostate from old animals. Outliers (O/Y > mean ± 2SD) were removed from the ratio calculation of the differentially expressed proteins. The identified tryptic peptide sequences of the differentially expressed proteins were BLAST searched against the Rat NCBI nr database to determine if they were unique entries or match to multiple members of a protein family and to obtain Entrez gene IDs. The differentially expressed proteins were then classified using the PANTHER Classification System (www.panther.com) based on their unique gene IDs. Pathway analyses were performed based on literature searches using Ingenuity Pathway Analysis software (Ingenuity Systems, CA) with the unique gene IDs as input to map the differentially expressed proteins to biological pathways.

Western blot analysis

Western blot analyses were performed on individual animals (Y, n = 4 and O, n = 3), which were pooled for ICAT experiment, and on an independent group of animals [3 month (n = 6); 12 month (n = 6); 16 month (n = 6)]. Fifty μg of total protein were electrophoresed on a 12% Criterion ready gel (Biorad, CA) and transferred onto a PVDF membrane (Immobilon FL, Millipore, MA) using a semi-dry Transblot SD cell at 23 V for 1.5 h (Biorad CV). Primary antibodies were used with the following conditions: 1:1000, 1 hr at room temperature for goat anti-rat glutathione S-transferase (GST) mu isoform (Oxford Biomedical Research, MI); 1:1000, 1 hr at room temperature for rabbit polyclonal ferritin (reacts with human, mouse and rat; Abcam, MA); 1:100, overnight at 4°C for rabbit polyclonal clusterin-α (reacts with mouse, rat and human, Santa Claus, CA); 1:1000, 1 hr at room temperature for cyclophilin B (CyPB; reacts with dog, human, chicken, mouse and rat; Abcam, MA); 1:500, overnight at 4°C for chicken spermine synthase (reacts with human, mouse and rat; Genway, CA); 1:200, overnight at 4°C for goat kininogen (reacts with rat, Santa Cruz, CA); 1:500, overnight at 4°C for ADP ribosylation factor (reacts with human, rat, mouse, dog and hamster; detect isoforms 1,3,5,6, but with ten fold reduction for isoform 4; Abcam, MA); 1:200, overnight at 4°C for oxygen regulated protein 150 (ORP150; react with rat), and 1:5000, 1 hr at room temperature for mouse monoclonal actin (reacts with many species, including rat, Abcam, MA). Corresponding IRDye™ conjugated secondary antibodies (Rockland, PA) were used at 1:5000 dilutions. Quantifications were performed with infrared detection using the software Odyssey v1.2 (LI-COR, NE). Two-tail Student's t-Test was performed using Excel.

RESULTS

Age-dependent decline in testosterone levels

Aging of male rats of different strains is associated with a decline in circulating testosterone [2]; however, this phenomenon has not been documented in the Noble rats. We measured

serum testosterone levels by a RIA in Noble rats with ages ranging from 4 months to 16 months and an age-dependent decline in testosterone levels was found (Figure 1). Worthy of mentioning is the compressed lifespan of this rat strain [24], which usually lives less than two years. The mean serum testosterone levels dropped from 3.45±0.66 ng/ml (mean ± SEM) in 4-month-old rats to 2.71±0.31 ng/ml at the age of 5-months, and further declined to 1.174±0.28 ng/ml at 9-months. Serum testosterone levels remained steady at 1.175±0.32 ng/ml in 16-month old animals.

Total number of protein identifications and false positive rate determination

To determine the number of protein identifications in all the 38 gel bands, we incorporated the search results of the LC/MS data derived from the 38 individual gel bands into three Multiple Consensus Reports in Bioworks 3.3, as the program allows an incorporation of only 15 search files into a single consensus report. We used XCorr [1.5(1+), 2.0(2+), 2.5(3+)] and ΔCN (=/>0.1) as protein identification criteria and limited the FP rate in each consensus report to less than 1% using a reverse database. Three hundred and fifty one proteins were identified in Multiple Consensus Report 1 (gel bands 36,37,38 and 1–12; MW 42.7 – 240 kD) [0.80% FP, P(pro) cut-off = 1.89×10^{-4}], 278 were identified in Multiple Consensus Report 2 (gel bands 13–26, MW 16.1 – ~40 kD) [0.72% FP, P(pro) cut-off = 8.19×10^{-6}], and 37 in Multiple Consensus Report 3 (gel bands 27–35, ~5 –15 kD) [0% FP, P(pro) cut-off = 5.22×10^{-6}], amounting to a total of 472 non-redundant protein identifications (Supplementary Table S1).

Number of differentially expressed proteins identified

Among the 472 proteins identified, 34 (7.2%) were found to be differentially expressed (median: > 2 fold and < 0.58) in the VP of old animals and with a CV of less than 45% for expression ratio of peptides in their respective proteins (Supplementary Table S2 and S3). Each protein was identified as a single unique entry in the NCBI nr protein database, expect T-kininogen I/II, hypothetical protein LOC306934/ferritin light chain, ADP-ribosylation factor 4/5, and alpha actinin 1/2/3 for which the identified sequences are common to the stated isoforms (Table 1a and 1b). Six entries of the differentially expressed proteins are predicted sequences that share sequence homology with the corresponding proteins of other species. Although the differentially expressed proteins identified have a low sequence coverage [2 % (protein disulfide-isomerase precursor) – 37% (GST-mu 3)] and 59% of them are single-peptide-based protein identifications (provided the fact that only cysteine containing peptides were targeted), most of them have a theoretical molecular weight in agreement with the molecular weight range of the gel bands from which they were identified. Details of peptide identification for all the differentially expressed proteins are summarized in Supplementary Table S4. Supplementary Table S6 lists all the single-peptide-based protein identifications with their sequence identified and scores [XCorr, P(pep) and ΔCN] Annotated MSMS spectra for all single-peptide-based protein identification are included in Supplementary Figure S1.

Age-dependent protein changes in the VP

Identified proteins deemed to be differentially expressed fall into a number of important functional categories (Tables 1a and 1b), including OS/detoxification [6 proteins: e.g.

glutathione S-transferase (GST Mu1 and 3; there were only modest increases in the expression of the other three isoforms (GST mu 2, 5 and 7 O/Y: 1.24, 1.70, 1.28, respectively; Supplementary Table S1), cystathionine beta-synthase, ferritin heavy and light chain], protein folding (5 proteins: e.g. Peptidyl-prolyl cis-trans isomerase B, HSP40, HSP86, hypoxia up-regulated 1), metabolism (10 proteins: e.g. heterogeneous nuclear ribonucleoprotein R, S-adenosylmethionine synthetase isoform type-2, glutamyl-prolyl-tRNA synthetase, eukaryotic translation initiation factor 2, subunit 1 alpha, ribosomal protein L36, spermidine synthase, hydroxymethylglutaryl-Co A synthase) and vesicle transport/intracellular trafficking/cytoskeleton (4 proteins: e.g. Transmembrane emp24 protein transport domain containing 9, ADP-ribosylation factor 4/5). Other identified proteins included a protease inhibitor (T-kininogen I/II), those related to cell signaling (2 proteins: Sel1h homolog and serine/threonine-protein phosphatase PP1-b), immune reaction (2 proteins: beta-defensin 50 and Ig kappa chain C region, B allele) and protein-lipid modification (palmitoyl-protein thioesterase 1).

Verification of protein expression levels by Western blot analysis

Among the 34 differentially expressed proteins, only 10 have an antibody commercially available (see Table 1, highlighted) and not all of the antibodies were suitable for Western blotting. After careful evaluation of the specificity of the antibodies for Western blotting we chose to purchase eight of them (including clusterin) to validate our targets. Verification of expression levels was performed on GST Mu, ferritin, cyclophilin B, spermine synthase, kininogen, ADP ribosylation factor, oxygen regulated protein 150 as well as clusterin using Western blot analyses on samples derived from the original 4 young and 3 old rats, which were pooled for the ICAT experiment, along with those obtained from an independent group of animals comprised of three age groups each with six animals [3 month (n = 6); 12 month (n = 6); 16 month (n = 6)] (Figure 3). As compared to 3 month old animals, the expression of GST-mu, ferritin, and clusterin was significantly increased in the VPs from 12-month and 16-month old animals [GST: 1.8 fold (3 mo. vs. 12 mo., $p < 0.01$), 1.9 fold (3 mo. vs. 16 mo., $p < 0.01$); ferritin: 2.3 fold (3 mo. vs. 12 mo., $p < 0.01$), 4.6 fold (3 mo. vs. 16 mo., $p < 0.01$), 2.0 fold (12 mo. vs. 16 mo., $p < 0.01$); clusterin: 1.5 fold (3 mo. vs. 12 mo., $p < 0.01$), 1.8 fold (3 mo. vs. 16 mo., $p < 0.01$)], and there was a significant increase in kininogen expression in 16-month old animals [3.4 fold (3 mo. Vs. 16 mo.), $p < 0.01$; 2.9 fold (12 mo. vs. 16 mo., $p < 0.01$)]. In contrast, ORP150, spermine synthase, cyclophilin B, and ADP-ribosylation factor showed an age-dependent decrease in expression in old animals [ORP150: 0.4 fold (3 mo. vs. 12 mo., $p < 0.01$), 0.1 fold (3 mo. vs. 16 mo., $p < 0.01$), 0.2 fold (12 mo. vs. 16 mo., $p < 0.01$); spermine synthase: 0.4 fold (3 mo. vs. 16 mo., $p < 0.01$), 0.4 fold (12 mo. vs. 16 mo., $p < 0.01$); cyclophilin B, 0.3 fold (3 mo. vs. 12 mo., $p < 0.01$), 0.2 fold (3 mo. vs. 16 mo., $p < 0.01$); ADP ribosylation factor: 0.6 fold (3 mo. vs. 16 mo., $p < 0.05$), 0.6 fold (12 mo. vs. 16 mo., $p < 0.05$)]. β-actin expression has a non statistically significant 1.2 fold increase in 16- month vs. 3- month old animals.

Correlation of expression levels

When comparing the proteomic data obtained in this study with that obtained from our previous gene profiling study [8], five proteins were found to be differentially expressed at the messenger level (Figure 4A). The mRNA and protein expression were found to be

decreased in spermidine synthase [gene expression: O/Y = 0.13; protein expression (ICAT): O/Y = 0.62)], protein disulfide-isomerase, prolyl-4-hydroxyl-β peptide [gene expression: O/Y = 0.16; protein expression (ICAT): O/Y =0.48], and found to be increased for clusterin [gene expression (microarray) O/Y = 3.4; gene expression (real-time PCR): O/Y = 2; protein expression (ICAT): O/Y = 2.99]. In contrast, ferritin heavy chain was increased at the protein level and decreased at the transcript level [protein expression (ICAT): O/Y = 3.26; gene expression: O/Y = 0.63] whereas S-adenosylmethionine synthetase was found to be decreased at the transcript level but increased at the protein level [gene expression (microarray) O/Y = 0.37; protein expression (ICAT): O/Y = 2.47].

Western blot results are in agreement with those obtained from the ICAT profiling for all the differentially expressed proteins for which an antibody is available and selected for Western analyses (Figure 4B). These include those identified by a single peptide (clusterin, ferritin, spermine synthase, cyclophilin B and ADP ribosylation factor). The increased clusterin protein levels are in agreement with the fact that clusterin is up-regulated at the transcription level in the aged Noble rat VP [8]. The fold change of decrease in expression levels of ADP ribosylation factor demonstrated by Western blot analysis in 16 mo. old versus 3 mo. old VP (0.6 fold, $p < 0.05$), which was different in magnitude from that obtained from the ICAT experiment (0.35 fold), may be accounted for by the specificity of the antibody used (which detects isoforms 1,3,5,6, but with a ten-fold reduction for isoform 4).

The extracted ion chromatograms and the zoom scan of the representative ICAT pair for β-actin (KLCYVALDFEQEMATAASSSSLEK) are shown in Figure 4C. The light and heavy labeled peptides of β-actin eluted at the same time (51.5 min). The zoom scan exhibits a pair of charge state-matched isotopomers with correct precursor masses [1360.5 (2+) and 1365 (2+)], showing O/Y ratio of 1.1 for β-actin. Supplementary Table S5 summarizes all the measurements (O/Y) for β-actin peptides sequenced. After averaging all the measurements (18 measurements of two unique peptides; with outliers removed), the O/Y ratio is 1.20, which is in agreement with the Western blot result (O/Y = 1.2).

Knowledge-based pathway analysis of the differentially expressed proteins

A literature-based pathway analysis software was used to investigate probable connections between the differentially expressed proteins. Twenty-two of the 34 differentially expressed proteins were mapped to 2 networks based on gene ontogeny and functionality (Figure 5). These networks are 1) cell-to-cell signaling and interaction/cell growth and connective tissue (Figure 5a, score 28; focus gene 14; 12 proteins) and, 2) cellular compromise, cellular function and maintenance, cell signaling (Figure. 5b, score 28; focus gene 14; 10 proteins). One distinct inferred network node, TNF-, was identified in network 1 (Fig. 5a). Six differentially expressed proteins are directly connected to TNF-α, including ARF4 (ADP-ribosylation factor 4), MAT2A (S-adenosylmethionine synthetase isoform type-2), FTH1 (ferritin, heavy polypeptide 1), P4HB (protein disulfide-isomerase precursor), EIF2S1 (eukaryotic translation initiation factor 2, subunit 1 alpha), and CBS (Isoform I of cystathionine beta-synthase).

DISCUSSION

In this study, using ICAT quantitative proteomic profiling, we identified 472 proteins with 34 exhibiting differential expression in the proteomes of the VPs from aged Noble rats versus their young counterparts. Notably, there is increased expression of proteins related to OS/detoxification, as well as a decrease in expression of proteins involved in protein folding, protein synthesis machinery, and cytoskeleton organization in the VP of old versus young Noble rats. The functional classes of proteins showing expression changes are in agreement with those identified from our previous transcriptional profiling experiments [8]. However, only a few of the differentially expressed proteins detected here were also found to have concordant changes in transcript levels in our previous transcriptome study [8]. The small number of concordant protein-transcript changes uncovered by these two studies is primarily due to the limited number of probes on the gene microarrays used in our transcriptome study (2,388 probes, MICROMAX microarray, Perkin Elmer). Nevertheless, clusterin, spermidine synthase, protein disulfide-isomerase, and prolyl-4-hydroxyl-β peptide were found to be altered in a concordant manner at both mRNA and protein levels in the aged VP (Figure 4a). The fact that mRNA levels do not necessarily correlate with protein expression is illustrated by the discrepancy in mRNA and protein levels for ferritin and S-adenosylmethionine synthetase. The latter finding is not surprising in light of the results from an integrative analysis of proteomic alterations and transcriptomic changes in prostate cancer specimens showing only 48%-64% concordance between protein and transcript levels [32].

One of the strengths of this study is that we have validated differential protein expression by Western blotting in an independent set of rats comprised of three age-groups, with six animals in each group, in addition to the 4 young and 3 old animals used in the ICAT experiment. The fact that all eight proteins selected for validation based on antibody availability were confirmed lends additional credence to the ICAT approach.

OS is believed to be a contributing factor to cellular aging [33] and the expression of specific antioxidant enzymes and redox-related proteins has been reported to be altered in the aged prostate [8–10]. In this study we found that four isoforms of GST mu, and cystathionine beta-synthase were up-regulated in the aged VPs of Noble rats. By their unique peptide sequences, GST-mu 1 and 3 were identified as having a 2-fold increase in expression in the aged VP, while there were only modest increases in the expression of the other three isoforms (GST mu 2, 5 and 7). GST activity is pivotal for the detoxification of electrophilic metabolites which, if not disposed of, may induce OS via redox cycling. The increased expression of cystathionine beta-synthase, which plays a key role in homocysteine and glutathione metabolism, is in agreement with the previous observation that cystathionine beta-synthase is up-regulated in the liver and brain of old animals [34, 35]. Up-regulation of these proteins may represent heightened cellular protective mechanisms in the aged prostate against OS. The disruption of redox balance in the aged gland is further supported by increased levels of ferritin, which is responsible for ion transport within the cells. Ferritin has been demonstrated to accumulate in tissues of aged rats and believed to compensate for the OS induced by an increase in iron concentrations in aged tissues [36, 37]. Another protein belonging to the ROS detoxification category that was identified with differential

expression was palmitoyl-protein thioesterase 1, which is a lysosomal enzyme that plays a role in the removal of fatty acids from lipid-modified proteins. Its increased expression may be a response to the accumulation of lipofuscin deposits [38] commonly observed in the aged VP of rats [9] as a result of insufficient detoxification systems [38]. Lastly, clusterin, a widely distributed glycoprotein whose biological functions include protection against OS-induced cell injury, was found to be up-regulated in the aged VP. Expression of this protein/gene was dramatically increased during androgen deprivation-induced prostatic epithelial involution [39]. However, we [40] and others [41] have provided evidence that clusterin up-regulation in prostatic cells is likely triggered by cellular OS damages rather than a loss of androgen suppression.

In our previous gene array study [8] two heat shock protein transcripts, BiP (GRP78) and tra1 (gp96), were found to be decreased in aged VPs. In the present study, decreased expression was found for a group of chaperone proteins (cyclophilin B, HSP40, HSP86, and ORP150). Cyclophilin B (CyPB) is a member of the immunophilin family of proteins [42] and serves as a chaperone in protein transport through the endoplasmic reticulum (ER) [43]. In breast epithelial cells, prolactin was shown to form a complex with CyPB and attain retrotranslocation to the nucleus to exert its action [44]. Although the rat prostate is sensitive to prolactin regulation, a similar role for CyPB has not been demonstrated for prostate cells. HSP40 protein has been recently shown to defend against protein carbonylation and to act as a cochaperone with HSP70 [45]. Interestingly, HSP70, which elicits an anti-apoptotic function by interacting with components of apoptotic pathways [46, 47], was found to be up-regulated in the dorsolateral lobe of the ACI rat prostate [22]. Besides acting as a chaperone, HSP40 may be involved in the regulation of eukaryotic initiation factor 2 alpha (eIF-2alpha)-mediated protein synthesis [48] and its reduced expression may represent an unfolded protein response to the accumulation of aggregated proteins in the ER. ORP150, alternatively known as hypoxia up-regulated 1 (HYOU1), is a heat shock protein 70-like protein that resides in the ER [49]. It suppresses hypoxia-induced apoptotic cell death [50] and its reduced expression by antisense treatment exerts antitumor-effects via VEGF suppression [51]. It was found to be androgen-dependent in the VP [52], although its role in aging is unknown. Overall, decreased expression in chaperone proteins may compromise intracellular protein trafficking, protection of the cell against cellular stress caused by protein misfolding [53], or the capacity for the removal of misfolded proteins [54], thus leading to senescence.

Aging is often accompanied by a decrease in protein metabolism in multiple tissues [55]. Glutamyl-prolyl-tRNA synthetase, eukaryotic translation initiation factor 2 and ribosomal protein L36, are all involved in protein biosynthesis and their expression was found to be decreased in the VP of aged animals. Cellular aging has also been suggested to be associated with reduced protein catabolism, which may involve inhibition of protease activity [56]. A 2- to 3-fold increase in T-kininogen expression, an inhibitor of cysteine proteinases, was observed in the aged VPs. This observation is in agreement with studies demonstrating that kininogen is a marker for aging in rats [57]. Additionally, kininogen has been shown to stimulate endothelial cell proliferation via ERK/AKT activation [58], and their increased levels may contribute in part to the proliferative characteristics of the aged prostate.

As demonstrated for mRNA in our microarray analysis [8], several proteins (ADP ribosyltransferase factor 1, glucosamine 6-phosphate N-acetyltransferase and alpha actinin) responsible for vesicle transport, intracellular trafficking and cytoskeleton organization were found to be diminished in aged VPs at the protein level. The messenger levels of ADP ribosyltransferase factor 1, which is involved in vesicle-mediated transport, was previously demonstrated to be decreased in the VP in old animals [8]. Glucosamine 6-phosphate N-acetyltransferase is involved in the biosynthesis of UDP-GlcNAc, which is critical for the initiation of protein glycosylation [59]. On the other hand, alpha actinin is involved in regulation of the cytoskeleton and serves as a scaffold to connect the cytoskeleton to diverse signaling pathways [60]. Polyamines play a paramount role in cell proliferation and chromatin stability [61, 62]. Altered expression of polyamines has been reported during aging and under pathological conditions such as cancer. In this study, reduced expression of spermidine synthase, a key enzyme in polyamine metabolism, was observed in the aged VP, suggesting a possibility of heightened risk of chromatin instability and relaxation of gene regulation in this tissue. This finding is in agreement with a previous report demonstrating reduced polyamine levels in the VP of rats older than 6-months [63]. The down-regulation of these proteins may lead to disruption of cell division and the histological features in the aged VP (atrophy and/or apoptotic activities of the luminal epithelial cells) as previously reported [8].

Several proteins, including Selh homolog, heterogeneous nuclear ribonucleoprotein R, beta-defensin 50, predicted proline rich 6 and esterase D/formylglutathione hydrolase were identified as differentially expressed between the young and old VP; however, their functions are unknown in the prostate. Worth noting is that the expression of Sel (suppressor-enhancer-lin) 1 homolog, named after the *C. elegans sel-1* gene product, is increased in the VP of aged Noble rats. Sel-1 protein is a negative regulator of the lin-12/Notch gene product, and eukaryotic Sel1 proteins are involved in endoplasmic reticulum-associated protein degradation and the unfolded protein response. Sel1 protein is activated under cellular stress [64] and has been implicated to play important roles in tumor development in the breast, pancreas and prostate [65, 66], possibly involving cell-matrix interaction.

Knowledge-based pathway analyses of prostatic proteins associated with aging revealed a connection of six proteins (ARF4, MAT2A, FTH1, P4HB, EIF2S1, and CBS) to a distinct inferred functional node, TNFα. TNFα is an inflammatory cytokine and the activation of its signaling, which leads to apoptosis, has been postulated as one of the aging mechanisms in other tissues [67, 68]. Its involvement in aging of the rat prostate is in agreement with the pro-inflammatory state observed in the prostates of elderly men [69, 70].

Finally, many of the changes in protein expression observed in the aging VP could be explained by dramatic changes in the morphology and function of the aged gland. As testosterone declines with aging, the prostatic epithelium undergoes atrophy and secretory function stops. These changes have been described in our previous study [8] and they clearly could have an impact on the expression of some of the aforementioned proteins. Alternatively, some of these proteins may be direct targets of androgen action. In this regard, we observed circulating testosterone levels in the 16-month old animals reduced to be one-

third of those in the young rats (3-month old). This magnitude of reduction has been observed in other rat strains with advancing age.

Taken together, in the aged prostate, significant changes occur in ROS metabolism with diminished levels of proteins related to protein folding, protein synthesis machinery and intracellular trafficking. The elevated OS is likely to be contributed to by the infiltration of inflammatory cells as previously observed in the aged VP [8] or reduction in androgen support as previously reported in a castration/androgen replacement experiment [40]. The increase in susceptibility to OS induced-protein modifications, together with a decline in protein fidelity maintenance and efficiency in removing damaged proteins, may lead to cellular senescence in the aged prostate. The mechanistic links between the above-mentioned differentially expressed proteins and aging prostate, testosterone decline, and disease development warrant further investigation. Mass spectrometry-based proteomic techniques serve as excellent tools to explore changes in the global protein profile, especially when the availability of antibodies is limited, as in our situation when working with a rat model, allowing a more comprehensive analysis of the diseased proteome.

Supplementary Material

Refer to Web version on PubMed Central for supplementary material.

Acknowledgments

This research was supported in part by NCI grants CA112532 and CA15776 awarded to SMH. We would like to thank Barbara Evans, Sonia Godoy-Tundidor and Suresh Cugativishweshwaraiah for reading the manuscript.

Abbreviations

CyPB	cyclophilin B
ER	endoplasmic reticulum
DLP	dorsolateral prostate
GST	glutathione S-transferase
HSP	heat shock protein
ORP150/HYOU1	oxygen regulated protein 150
O/Y	old/young
OS	oxidative stress
RIA	radioimmunoassay
TNFα	tumor necrosis factor-α
TRPM2	clusterin
VP	ventral prostate

References

1. Hsing AW, Tsao L, Devesa SS. International trends and patterns of prostate cancer incidence and mortality. Int J Cancer. 2000; 85:60–67. [PubMed: 10585584]
2. Isaacs JT. The aging ACI/Seg versus Copenhagen male rat as a model system for the study of prostatic carcinogenesis. Cancer Res. 1984; 44:5785–5796. [PubMed: 6498839]
3. Malins DC, Johnson PM, Wheeler TM, Barker EA, et al. Age-related radical-induced DNA damage is linked to prostate cancer. Cancer Res. 2001; 61:6025–6028. [PubMed: 11507046]
4. Banerjee S, Banerjee PP, Brown TR. Castration-induced apoptotic cell death in the Brown Norway rat prostate decreases as a function of age. Endocrinology. 2000; 141:821–832. [PubMed: 10650965]
5. Anim JT, Udo C, John B. Characterisation of inflammatory cells in benign prostatic hyperplasia. Acta Histochem. 1998; 100:439–449. [PubMed: 9842422]
6. Banu NA, Azim FA, Kamal M, Rumi MA, et al. Inflammation and glandular proliferation in hyperplastic prostates: association with prostate specific antigen value. Bangladesh Med Res Counc Bull. 2001; 27:79–83. [PubMed: 12197626]
7. De Marzo AM, Marchi VL, Epstein JI, Nelson WG. Proliferative inflammatory atrophy of the prostate: implications for prostatic carcinogenesis. Am J Pathol. 1999; 155:1985–1992. [PubMed: 10595928]
8. Lau KM, Tam NN, Thompson C, Cheng RY, et al. Age-associated changes in histology and gene-expression profile in the rat ventral prostate. Lab Invest. 2003; 83:743–757. [PubMed: 12746483]
9. Morrissey C, Buser A, Scolaro J, O'Sullivan J, et al. Changes in hormone sensitivity in the ventral prostate of aging Sprague-Dawley rats. J Androl. 2002; 23:341–351. [PubMed: 12002436]
10. Suzuki K, Oberley TD, Pugh TD, Sempf JM, Weindruch R. Caloric restriction diminishes the age-associated loss of immunoreactive catalase in rat prostate. Prostate. 1997; 33:256–263. [PubMed: 9397198]
11. Banerjee PP, Banerjee S, Brown TR. Increased androgen receptor expression correlates with development of age-dependent, lobe-specific spontaneous hyperplasia of the brown Norway rat prostate. Endocrinology. 2001; 142:4066–4075. [PubMed: 11517186]
12. Giri D, Ozen M, Ittmann M. Interleukin-6 is an autocrine growth factor in human prostate cancer. Am J Pathol. 2001; 159:2159–2165. [PubMed: 11733366]
13. Harkonen PL, Makela SI, Valve EM, Karhukorpi EK, Vaananen HK. Differential regulation of carbonic anhydrase II by androgen and estrogen in dorsal and lateral prostate of the rat. Endocrinology. 1991; 128:3219–3227. [PubMed: 1903702]
14. Prins GS, Jung MH, Vellanoweth RL, Chatterjee B, Roy AK. Age-dependent expression of the androgen receptor gene in the prostate and its implication in glandular differentiation and hyperplasia. Dev Genet. 1996; 18:99–106. [PubMed: 8934871]
15. Ruffion A, Al Sakkaf KA, Brown BL, Eaton CL, et al. The survival effect of prolactin on PC3 prostate cancer cells. Eur Urol. 2003; 43:301–308. [PubMed: 12600435]
16. Sanchez-Visconti G, Herrero L, Rabadan M, Pereira I, Ruiz-Torres A. Ageing and prostate: age-related changes in androgen receptors of epithelial cells from benign hypertrophic glands compared with cancer. Mech Ageing Dev. 1995; 82:19–29. [PubMed: 7475354]
17. Bhowmick NA, Chytil A, Plieth D, Gorska AE, et al. TGF-beta signaling in fibroblasts modulates the oncogenic potential of adjacent epithelia. Science. 2004; 303:848–851. [PubMed: 14764882]
18. Olumi AF, Grossfeld GD, Hayward SW, Carroll PR, et al. Carcinoma-associated fibroblasts direct tumor progression of initiated human prostatic epithelium. Cancer Res. 1999; 59:5002–5011. [PubMed: 10519415]
19. Parrinello S, Coppe JP, Krtolica A, Campisi J. Stromal-epithelial interactions in aging and cancer: senescent fibroblasts alter epithelial cell differentiation. J Cell Sci. 2005; 118:485–496. [PubMed: 15657080]
20. Bavik C, Coleman I, Dean JP, Knudsen B, et al. The gene expression program of prostate fibroblast senescence modulates neoplastic epithelial cell proliferation through paracrine mechanisms. Cancer Res. 2006; 66:794–802. [PubMed: 16424011]

21. Begley L, Monteleon C, Shah RB, Macdonald JW, Macoska JA. CXCL12 overexpression and secretion by aging fibroblasts enhance human prostate epithelial proliferation in vitro. Aging Cell. 2005; 4:291–298. [PubMed: 16300481]
22. Reyes I, Reyes N, Iatropoulos M, Mittelman A, Geliebter J. Aging-associated changes in gene expression in the ACI rat prostate: Implications for carcinogenesis. Prostate. 2005; 63:169–186. [PubMed: 15486989]
23. Yamashita S, Suzuki S, Nomoto T, Kondo Y, et al. Linkage and microarray analyses of susceptibility genes in ACI/Seg rats: a model for prostate cancers in the aged. Cancer Res. 2005; 65:2610–2616. [PubMed: 15805257]
24. Ho SM, Lane K. Sex hormone-induction and dietary modulation of prostatic adenocarcinoma (PA) in animal models. Urologic Oncology. 1996; 2:110–115. [PubMed: 21224149]
25. Everley PA, Bakalarski CE, Elias JE, Waghorne CG, et al. Enhanced analysis of metastatic prostate cancer using stable isotopes and high mass accuracy instrumentation. J Proteome Res. 2006; 5:1224–1231. [PubMed: 16674112]
26. Gygi SP, Rist B, Gerber SA, Turecek F, et al. Quantitative analysis of complex protein mixtures using isotope-coded affinity tags. Nat Biotechnol. 1999; 17:994–999. [PubMed: 10504701]
27. Meehan KL, Sadar MD. Quantitative profiling of LNCaP prostate cancer cells using isotope-coded affinity tags and mass spectrometry. Proteomics. 2004; 4:1116–1134. [PubMed: 15048993]
28. Wright ME, Eng J, Sherman J, Hockenbery DM, et al. Identification of androgen-coregulated protein networks from the microsomes of human prostate cancer cells. Genome Biol. 2003; 5:R4. [PubMed: 14709176]
29. Comuzzi B, Sadar MD. Proteomic analyses to identify novel therapeutic targets for the treatment of advanced prostate cancer. Cellscience. 2006; 3:61–81. [PubMed: 17205105]
30. Elias JE, Gibbons FD, King OD, Roth FP, Gygi SP. Intensity-based protein identification by machine learning from a library of tandem mass spectra. Nat Biotechnol. 2004; 22:214–219. [PubMed: 14730315]
31. Peng J, Elias JE, Thoreen CC, Licklider LJ, Gygi SP. Evaluation of multidimensional chromatography coupled with tandem mass spectrometry (LC/LC-MS/MS) for large-scale protein analysis: the yeast proteome. J Proteome Res. 2003; 2:43–50. [PubMed: 12643542]
32. Varambally S, Yu J, Laxman B, Rhodes DR, et al. Integrative genomic and proteomic analysis of prostate cancer reveals signatures of metastatic progression. Cancer Cell. 2005; 8:393–406. [PubMed: 16286247]
33. Davydov VV, Dobaeva NM, Bozhkov AI. Possible role of alteration of aldehyde's scavenger enzymes during aging. Exp Gerontol. 2004; 39:11–16. [PubMed: 14724059]
34. Ichinohe A, Kanaumi T, Takashima S, Enokido Y, et al. Cystathionine beta-synthase is enriched in the brains of Down's patients. Biochem Biophys Res Commun. 2005; 338:1547–1550. [PubMed: 16274669]
35. Nakata K, Kawase M, Ogino S, Kinoshita C, et al. Effects of age on levels of cysteine, glutathione and related enzyme activities in livers of mice and rats and an attempt to replenish hepatic glutathione level of mouse with cysteine derivatives. Mech Ageing Dev. 1996; 90:195–207. [PubMed: 8898313]
36. Choi JH, Kim DW, Yu B. Modulation of age-related alterations of iron, ferritin, and lipid peroxidation in rat brain synaptosomes. J Nutr Health Aging. 1998; 2:133–137. [PubMed: 10995054]
37. Dentchev T, Hahn P, Dunaief JL. Strong labeling for iron and the iron-handling proteins ferritin and ferroportin in the photoreceptor layer in age-related macular degeneration. Arch Ophthalmol. 2005; 123:1745–1746. [PubMed: 16344450]
38. Gems D, McElwee JJ. Broad spectrum detoxification: the major longevity assurance process regulated by insulin/IGF-1 signaling? Mech Ageing Dev. 2005; 126:381–387. [PubMed: 15664624]
39. Kyprianou N, Isaacs JT. Expression of transforming growth factor-beta in the rat ventral prostate during castration-induced programmed cell death. Mol Endocrinol. 1989; 3:1515–1522. [PubMed: 2608047]

40. Tam NN, Gao Y, Leung YK, Ho SM. Androgenic regulation of oxidative stress in the rat prostate: involvement of NAD(P)H oxidases and antioxidant defense machinery during prostatic involution and regrowth. Am J Pathol. 2003; 163:2513–2522. [PubMed: 14633623]
41. Miyake H, Hara I, Gleave ME, Eto H. Protection of androgen-dependent human prostate cancer cells from oxidative stress-induced DNA damage by overexpression of clusterin and its modulation by androgen. Prostate. 2004; 61:318–323. [PubMed: 15389725]
42. Allain F, Durieux S, Denys A, Carpentier M, Spik G. Cyclophilin B binding to platelets supports calcium-dependent adhesion to collagen. Blood. 1999; 94:976–983. [PubMed: 10419889]
43. Klappa P, Freedman RB, Zimmermann R. Protein disulphide isomerase and a lumenal cyclophilin-type peptidyl prolyl cis-trans isomerase are in transient contact with secretory proteins during late stages of translocation. Eur J Biochem. 1995; 232:755–764. [PubMed: 7588713]
44. Rycyzyn MA, Clevenger CV. The intranuclear prolactin/cyclophilin B complex as a transcriptional inducer. Proc Natl Acad Sci U S A. 2002; 99:6790–6795. [PubMed: 11997457]
45. Fredriksson A, Ballesteros M, Dukan S, Nystrom T. Defense against protein carbonylation by DnaK/DnaJ and proteases of the heat shock regulon. J Bacteriol. 2005; 187:4207–4213. [PubMed: 15937182]
46. Beere HM, Wolf BB, Cain K, Mosser DD, et al. Heat-shock protein 70 inhibits apoptosis by preventing recruitment of procaspase-9 to the Apaf-1 apoptosome. Nat Cell Biol. 2000; 2:469–475. [PubMed: 10934466]
47. Gurbuxani S, Schmitt E, Cande C, Parcellier A, et al. Heat shock protein 70 binding inhibits the nuclear import of apoptosis-inducing factor. Oncogene. 2003; 22:6669–6678. [PubMed: 14555980]
48. van Huizen R, Martindale JL, Gorospe M, Holbrook NJ. P58IPK, a novel endoplasmic reticulum stress-inducible protein and potential negative regulator of eIF2alpha signaling. J Biol Chem. 2003; 278:15558–64. [PubMed: 12601012]
49. Brocchieri L, Conway dM, Macario AJ. Chaperonomics, a new tool to study ageing and associated diseases. Mech Ageing Dev. 2007; 128:125–136. [PubMed: 17123587]
50. Ozawa K, Kuwabara K, Tamatani M, Takatsuji K, et al. 150-kDa oxygen-regulated protein (ORP150) suppresses hypoxia-induced apoptotic cell death. J Biol Chem. 1999; 274:6397–6404. [PubMed: 10037731]
51. Miyagi T, Hori O, Koshida K, Egawa M, et al. Antitumor effect of reduction of 150-kDa oxygen-regulated protein expression on human prostate cancer cells. Int J Urol. 2002; 9:577–585. [PubMed: 12445237]
52. Jiang F, Wang Z. Identification of androgen-responsive genes in the rat ventral prostate by complementary deoxyribonucleic acid subtraction and microarray. Endocrinology. 2003; 144:1257–1265. [PubMed: 12639908]
53. Proctor CJ, Soti C, Boys RJ, Gillespie CS, et al. Modelling the actions of chaperones and their role in ageing. Mech Ageing Dev. 2005; 126:119–131. [PubMed: 15610770]
54. Merker K, Grune T. Proteolysis of oxidised proteins and cellular senescence. Exp Gerontol. 2000; 35:779–786. [PubMed: 11053668]
55. Rattan SI. Protein synthesis and the components of protein synthetic machinery during cellular aging. Mutat Res. 1991; 256:115–125. [PubMed: 1722004]
56. Keppler D, Walter R, Perez C, Sierra F. Increased expression of mature cathepsin B in aging rat liver. Cell Tissue Res. 2000; 302:181–188. [PubMed: 11131129]
57. Acuna-Castillo C, Leiva-Salcedo E, Gomez CR, Perez V, et al. T-kininogen: a biomarker of aging in Fisher 344 rats with possible implications for the immune response. J Gerontol A Biol Sci Med Sci. 2006; 61:641–649. [PubMed: 16870624]
58. Perez V, Leiva-Salcedo E, Acuna-Castillo C, Aravena M, et al. T-kininogen induces endothelial cell proliferation. Mech Ageing Dev. 2006; 127:282–289. [PubMed: 16378635]
59. Boehmelt G, Wakeham A, Elia A, Sasaki T, et al. Decreased UDP-GlcNAc levels abrogate proliferation control in EMeg32-deficient cells. EMBO J. 2000; 19:5092–5104. [PubMed: 11013212]
60. Otey CA, Carpen O. Alpha-actinin revisited: a fresh look at an old player. Cell Motil Cytoskeleton. 2004; 58:104–111. [PubMed: 15083532]

61. Pollard KJ, Samuels ML, Crowley KA, Hansen JC, Peterson CL. Functional interaction between GCN5 and polyamines: a new role for core histone acetylation. EMBO J. 1999; 18:5622–5633. [PubMed: 10523306]

62. Hobbs CA, Gilmour SK. High levels of intracellular polyamines promote histone acetyltransferase activity resulting in chromatin hyperacetylation. J Cell Biochem. 2000; 77:345–360. [PubMed: 10760944]

63. Bettuzzi S, Strocchi P, Marinelli M, Astancolle S, et al. Gene relaxation and aging: changes in the abundance of rat ventral prostate SGP-2 (clusterin) and ornithine decarboxylase mRNAs. FEBS Lett. 1994; 348:255–258. [PubMed: 8034050]

64. Mittl PR, Schneider-Brachert W. Sel1-like repeat proteins in signal transduction. Cell Signal. 2007; 19:20–31. [PubMed: 16870393]

65. Cattaneo M, Orlandini S, Beghelli S, Moore PS, et al. SEL1L expression in pancreatic adenocarcinoma parallels SMAD4 expression and delays tumor growth in vitro and in vivo. Oncogene. 2003; 22:6359–6368. [PubMed: 14508516]

66. Orlandi R, Cattaneo M, Troglio F, Casalini P, et al. SEL1L expression decreases breast tumor cell aggressiveness in vivo and in vitro. Cancer Res. 2002; 62:567–574. [PubMed: 11809711]

67. Dirks AJ, Leeuwenburgh C. Tumor necrosis factor alpha signaling in skeletal muscle: effects of age and caloric restriction. J Nutr Biochem. 2006; 17:501–508. [PubMed: 16517142]

68. Gupta S, Gollapudi S. Molecular mechanisms of TNF-alpha-induced apoptosis in aging human T cell subsets. Int J Biochem Cell Biol. 2005; 37:1034–1042. [PubMed: 15743676]

69. Bruunsgaard H. Effects of tumor necrosis factor-alpha and interleukin-6 in elderly populations. Eur Cytokine Netw. 2002; 13:389–391. [PubMed: 12517724]

70. Maggio M, Basaria S, Ceda GP, Ble A, et al. The relationship between testosterone and molecular markers of inflammation in older men. J Endocrinol Invest. 2005; 28:116–119. [PubMed: 16760639]

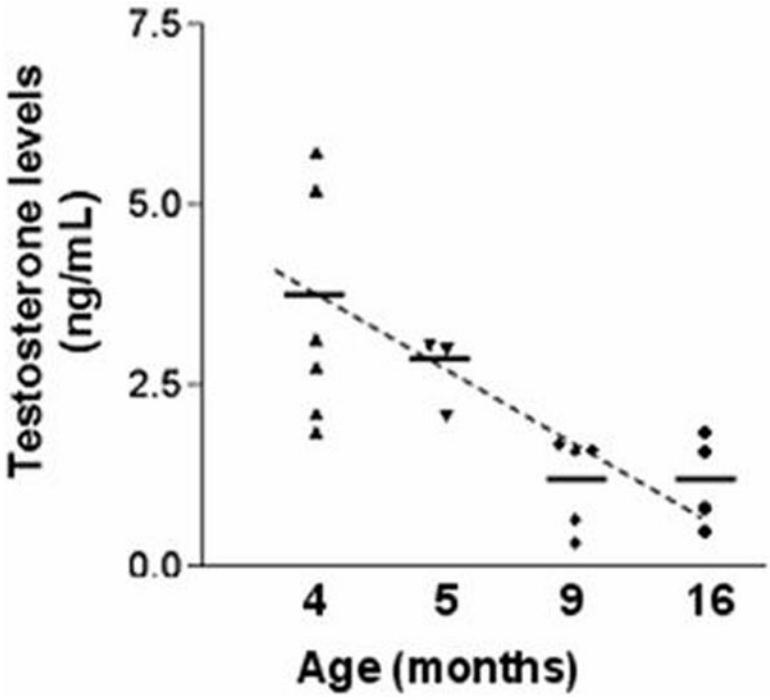

Figure 1. RIA of serum testosterone levels

Serum total testosterone levels from animals aged 4, 5, 9 and 16 months (n=3–6) were measured by RIA (Coat-A-Count Total Testosterone). The sensitivity of the assay was 0.04 ng/ml. RIA was performed according to the manufacturer's instructions. Each data point represents an average of two measurements obtained from one animal.

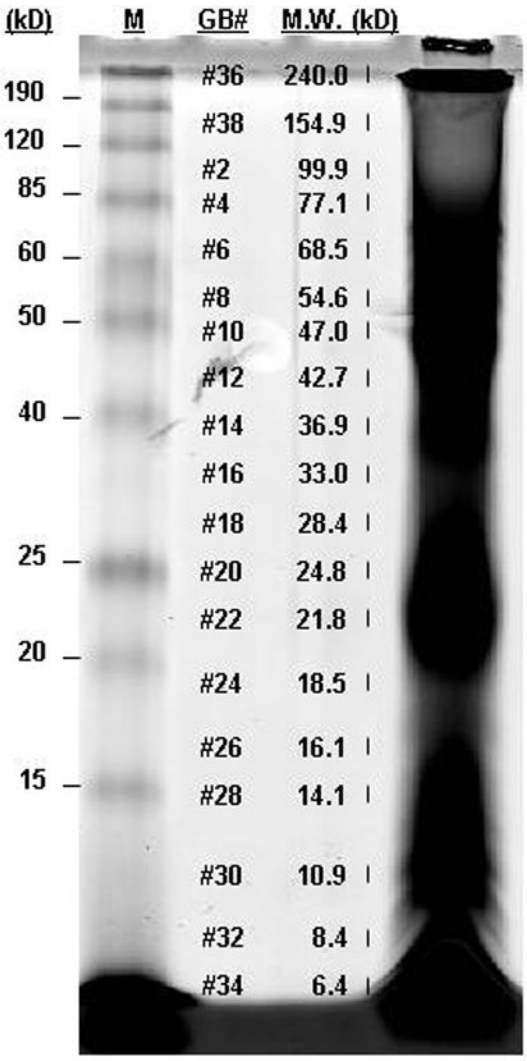

Figure 2. Gel-based separation of ICAT labeled proteins

One mg of “light” and “heavy” labeled proteins from 3-month-old and 16-month-old VPs, respectively, were combined and subjected to SDS-PAGE separation. The gel lane was excised into 38 bands. The MW of each gel band was determined with reference to a 10–200 kDa molecular weight marker. Each band was subjected to tryptic digestion and subsequent μLC/MS/MS analysis. M, molecular weight marker. GB#, gel band number. MW, molecular weight in kDa.

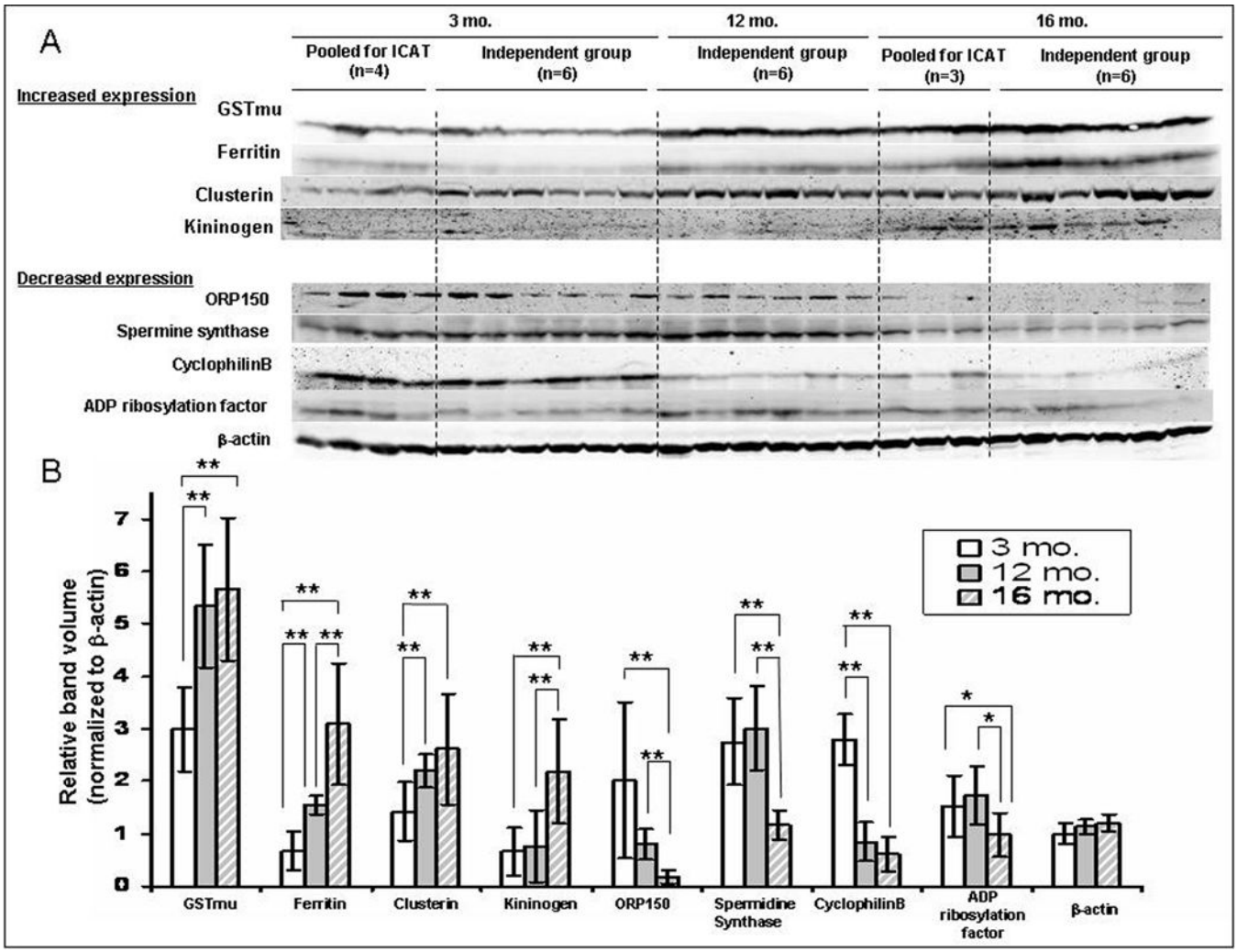

Figure 3. Verification of protein expression levels

A. Expression of GST-mu, ferritin, clusterin, kininogen, oxygen regulated protein 150, spermine synthase, cyclophilin B and ADP ribosylation factor were validated using Western blot in the VP of individual animals, which were pooled for ICAT experiment, as well as on an independent group of animals [3 month (n = 6); 12 month (n = 6); 16 month (n = 6)]. **B.** The densitometry demonstrated that all the proteins analyzed showed an age-dependent change in expression (normalized to β-actin expression; *, $p < 0.05$, **, $p < 0.01$).

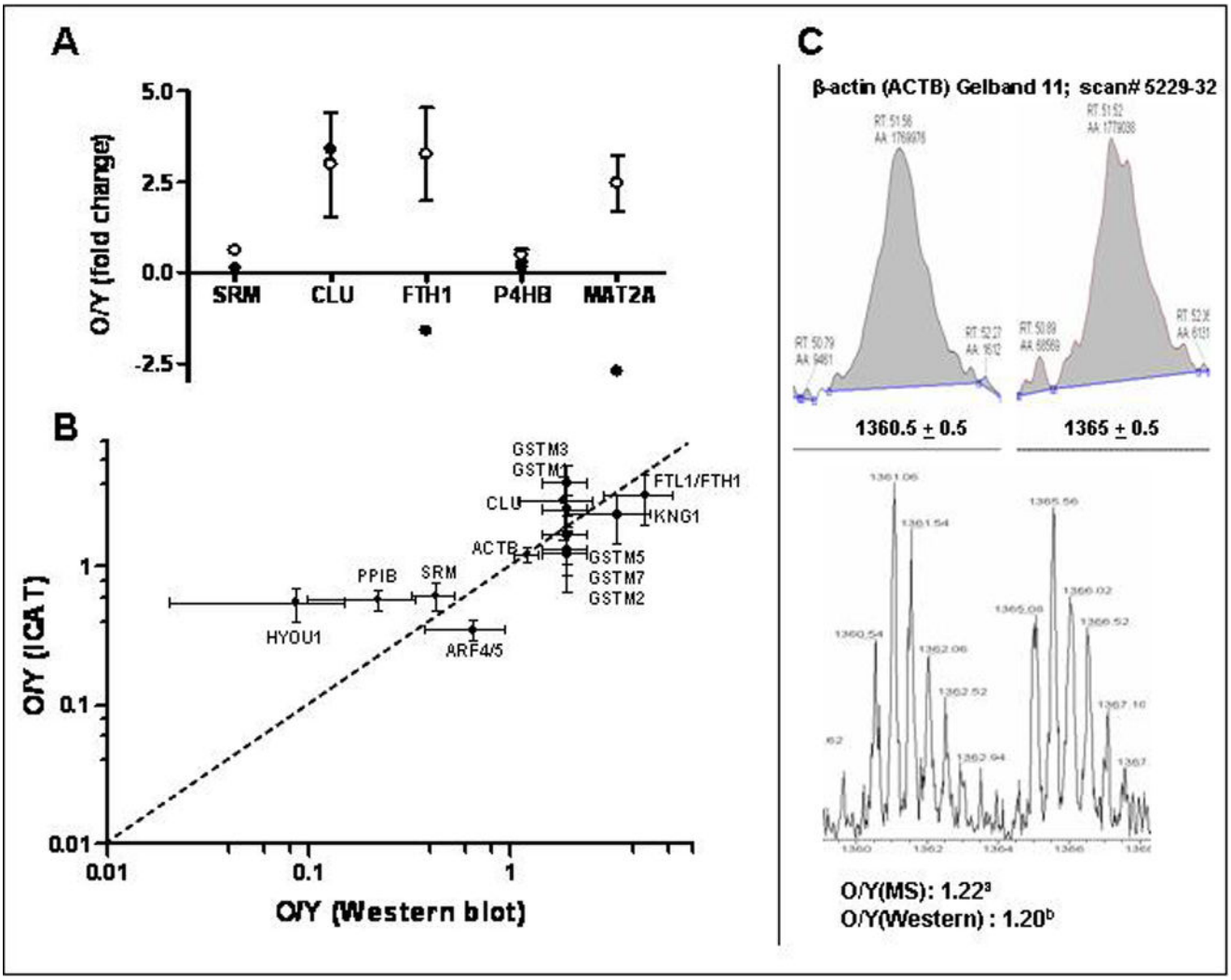

Figure 4. Correlation of expression data

A. Spermidine synthase (SRM), clusterin (CLU), ferritin heavy chain (FTH1), S-adenosylmethionine synthetas (MAT2A), and protein disulfide-isomerase, prolyl-4-hydroxyl-β peptide (P4HB) were found to be differentially expressed in our previous microarray study [8] and the present proteomics study. Closed circles (●) represent transcript levels and open circles (○) represent protein levels determined by ICAT-MS. Transcript levels are represented as mean with t-value of −2.2, 2.2, −2.0, −2.5, −2.6 for SRM, CLU, FTH1, P4HB and MAT2A, respectively [8] and protein levels represented as mean ± SD. **B.** Fold changes determined by Western blotting were plotted against those obtained from the ICAT-experiment for GST-mu, ferritin, clusterin, kininogen (KNG1/2), oxygen regulated protein 150, spermine synthase, cyclophilin B and ADP ribosylation factor and β-actin. All data points cluster around the central diagonal line. GSTmu1, 2, 3, 5 and 7 were included as the GST antibody recognizes all the mu isoforms. Only mu1 and 3 had an O/Y > 2. Values are represented by mean fold change (O/Y) ± SD. **C**. The light and heavy labeled peptides of β-actin eluted at the same time (51.5 min). Shown is the zoom scan of a representative pair of charge state-matched isotopomers for β-actin with correct precursor

masses [1360.5 (2+) and 1365 (2+)], showing O/Y ratios of 1.1 as demonstrated by the extracted ion chromatograms. **a)** O/Y(MS): O/Y of 1.22 was obtained from averaging all the measurements (18 measurements of two unique peptides; with outliers removed) for β-actin peptides sequenced (Supplementary S5). **b)**, O/Y (Western): O/Y of 1.20 was obtained from Figure 3.

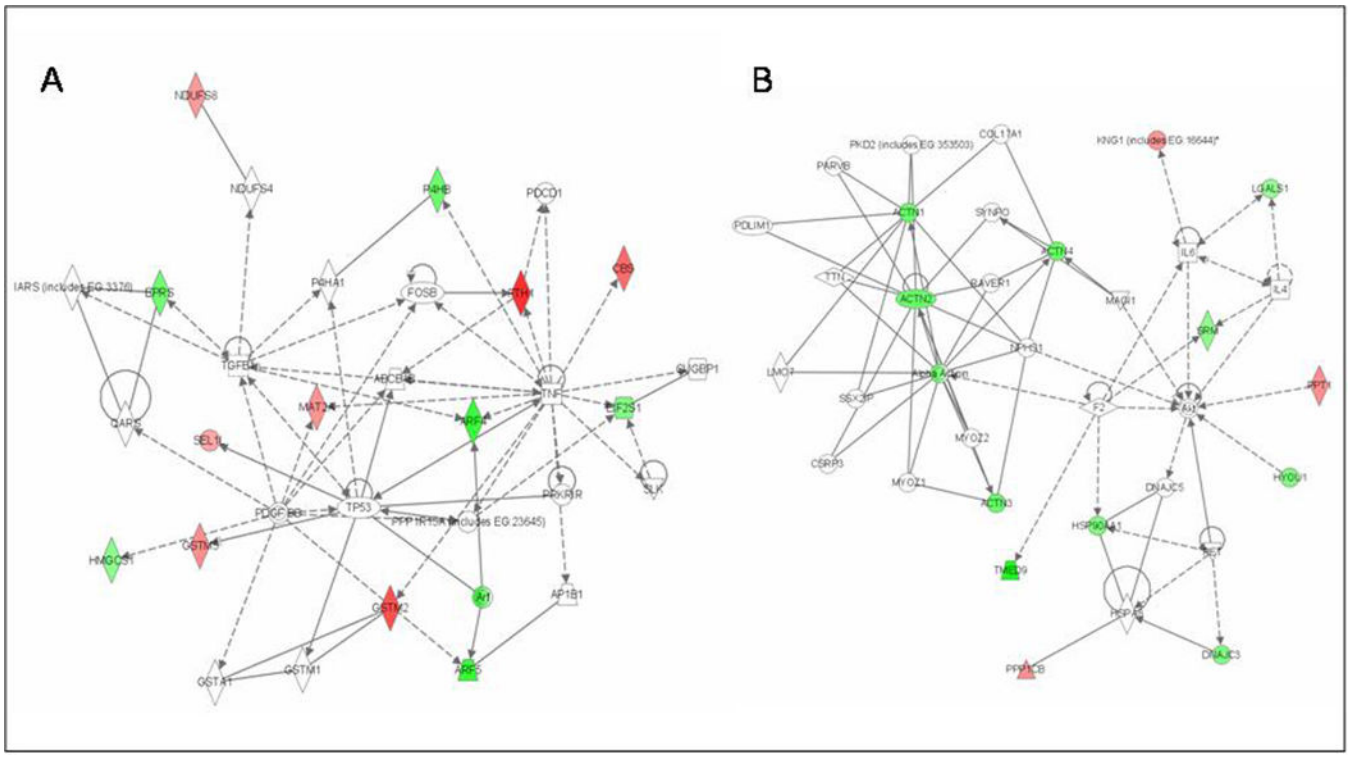

Figure 5. Knowledge-based Pathway analysis

Twenty-four of the differentially expressed proteins were principally mapped to 2 networks. **A)** Network 1: cell-to-cell signaling and interaction/cell growth and connective tissue (with 6 proteins directly connecting to one distinct inferred network node, TNF-α). **B)** Network 2: cellular compromise, cellular function and maintenance, cell signaling. Participating proteins are represented in the network by their Entrez Gene official symbols, with increased expression represented by red nodes and decreased expression by green nodes.

Table 1

a. Proteins with increased expression in the ventral prostate (VP) of 16-month-old animals										
IPI ID	**Gene Name**	**Protein Name**	**MW**	**GB#[a]**	**No. of Unique Peptide *b***	**Coverage (%)**	**No. of measurement for protein quantitation *c***	**O/Y (Mean)**	**O/Y (Median)**	**CV (%)[d]**
Detoxification/Oxidative stress										
IPI00231639.7	GSTM1	Glutathione S-transferase Mu 1[e]	25897	17–22	3	23	31	2.59	2.49	26
IPI00230942.5	GSTM3	Glutathione S-transferase Mu 3	25664	17,18,21–23	4	37	5	3.99	3.72	36
IPI00214299.6	CBS	Cystathionine beta-synthase	61327	1,5	1	5	3	3.65	2.91	35
IPI00382226.1 IPI00679203.3	RGD1306939 FTL1	Hypothetical protein LOC306934 (Ferritin_Like) Ferritin light chain	144619	22	1	1 11	2	2.53	2.53	3.1
IPI00373143.1	FTH1	*Ferritin heavy chain*	21019	22	1	13	1	4.73	4.73	–
IPI00371286.2	ASNA1	Predicted: Similar to ARSA (bacterial) arsenite transporter	38993	13	1	6	3	2.07	2.19	10
Cell Signaling										
IPI00205606.3	SEL1L	Sel1h Sel-1 homolog precursor	88627	25	1	3	3	1.98	1.97	0.87
IPI00203390.3	PPP1CB	Serine/threonine-protein phosphatase PP1-b catalytic subunit	37163	11,12	1	4	3	2.53	3.14	43
IPI00198667.7	CLU	Clusterin	51342	11,14,16,20	1	5	3	2.99	3.47	48
Protease inhibitor										
IPI00679245.1 IPI00327182.4	MGC108747 KNG1	T-kininogen II (Major acute phase protein) T-kininogen I	48076 47764	6	2	4	3	2.39	2.65	38.3
Protein-lipid modification										
IPI00208382.1	PPT1	Palmitoyl-protein thioesterase 1	34432	11–15	2	12	15	2.56	2.39	30
Metabolism										
IPI00372407.3	Apoa1bp_predicted	Predicted: similar to apolipoprotein A-I binding protein	30871	16–18	1	8	3	2.09	2.37	41
IPI00194562.3	HNRPR	Heterogeneous nuclear ribonucleoprotein R	70831	1,3	1	2	2	2.54	2.54	32
IPI00189991.1	MAT2A	*S-adenosylmethionine synthetase isoform type-2*[d]	43688	10–12	1	6	7	2.47	2.04	31
IPI00188850.3	RPIA_predicted	Predicted: Ribose-5-phosphate isomerase	32452	18,20	1	6	3	1.99	2.07	7.3
IPI00188330.1	NDUFS8_predicted	Predicted: NADH dehydrogenase (ubiquinone) Fe-S protein 8	23955	18	1	8	3	2.34	2.34	25
Immune response										
IPI00558849.1	DEFB50	Beta-defensin 50	7895	31, 32	1	32	2	2.32	2.32	21

a. Proteins with increased expression in the ventral prostate (VP) of 16-month-old animals										
IPI ID	**Gene Name**	**Protein Name**	**MW**	**GB#[a]**	**No. of Unique Peptide *b***	**Coverage (%)**	**No. of measurement for protein quantitation *c***	**O/Y (Mean)**	**O/Y (Median)**	**CV (%)[d]**
IPI00388002.2	LOC500180 LOC500183	Ig kappa chain	34455	15–17,20,22	1	7	10	3.72	3.58	18

b. Proteins with decreased expression in the VP of 16-month-old animals										
IPI ID	**Gene Name**	**Protein Name**	**MW**	**GB#**	**No. of unique Peptide *a***	**Coverage (%)**	**No. of measurement for protein quantitation[b]**	**O/Y (Mean)**	**O/Y (Median)**	**CV[c] (%)**
Protein folding										
IPI00213644.3	PPIB	Peptidyl-prolyl cis-trans isomerase B (Cyclophilin B)	23803	21,22	1	6	5	0.58	0.53	18
IPI00206660.2	DNAJC3	Protein kinase inhibitor p58, DnaJ (HSP40)C3 homolog	57563	3,5,6	2	7	11	0.57	0.58	22
IPI00210566.3	HSPCA	Heat shock protein HSP 1, alpha (HSP 86), HSP 90 alpha	84818	1–4	5	13	5	0.55	0.42	44
IPI00210975.1	HYOU1	150kDa oxygen-regulated protein, hypoxia up regulated protein 1	111291	38,1	2	2	3	0.55	0.57	27
IPI00198887.1	P4HB	Protein disulfide-isomerase, prolyl-4-hydroxyl -β peptide	56916	5–7,9–14,16,17	2	2	22	0.48	0.5	31
Metabolism										
IPI00421357.2	EPRS	Glutamyl-prolyl-tRNA synthetase	169980	1,6	2	4	3	0.49	0.43	41
IPI00230830.5	EIF2S1	Eukaryotic translation initiation factor 2 (eif-2) subunit 1 alpha	36086	12–14	1	5	6	0.57	0.55	20
IPI00206789.1	RPL36	Ribosomal protein L36 [Rattus norvegicus]	12219	27–29	1	8	4	0.54	0.53	18
IPI00197952.1	SRM	*Spermidine synthase*	33975	12–15	1	7	11	0.62	0.57	22
IPI00188158.1	HMGCS1	Hydroxymethylglutaryl-CoA synthase, cytoplasmic	57398	2,3,6	1	2	3	0.62	0.55	24
Vesicle transport/Intracellular trafficking/Cytoskeleton										
IPI00364707.1	TMED9	Transmembrane emp24 protein transport domain containing 9	27011	18	1	8	2	0.31	0.31	27
IPI00231965.5	ARF4 ARF5	ADP-ribosylation factor 4 ADP-ribosylation factor 5	20517	21,22	1	8	3	0.35	0.36	16
IPI00200773.1	ACTN1 ACTN2 ACTN3 ACTN4	Alpha-actinin alpha 1 Predicted similar to actinin alpha 2 Actinin alpha 3 Actinin alpha 4	102948	38,2,3,6	2	4	7	0.47	0.50	20
IPI00231275.7	LGALS1	Beta-galactoside-binding lectin (galectin)	14847	25	2	20	5	0.66	0.57	18
Miscellaneous										

b. Proteins with decreased expression in the VP of 16-month-old animals										
IPI ID	**Gene Name**	**Protein Name**	**MW**	**GB#**	**No. of unique Peptide *a***	**Coverage (%)**	**No. of measurement for protein quantitation*b***	**O/Y (Mean)**	**O/Y (Median)**	**CV*c* (%)**
IPI00198604.2	RGD1563144_predicted	Preducted_similar to glucosamine 6-phosphate N-acetyltransferase	42849	20–22	2	8	4	0.44	0.36	43
IPI00197723.4	RGD1565681_predicted	Predicted similar to proline rich 6	27499	14,15	1	4	2	0.58	0.58	22
IPI00362395.4	Esd	Esterase D/formylglutathione hydrolase	31543	13,14	2	14	3	0.49	0.49	37

a) Number of unique peptides (same amino acid sequence that may have modification (heavy/light labeled, oxidation) identified according to the criteria of XCorr values of 1.5 (1+), 2.0 (2+) and 2.5 (3+), DelCN =/> 0.1, and two missed cleavages allowed. Detailed information regarding peptide identification of the differentially expressed proteins is included in Supplementary Table S4.

b) Number of quantifiable peptides used in ratio calculation: peptides that have labeled cysteines (including those with modification and/or were measured repeatedly).

c) CV (%): coefficient of variation = standard deviation/mean. CVs (%) were calculated for proteins having 2 or more quantifiable peptides.

d) Proteins whose transcript was found to be differentially expressed in our previous microarray study were italiced.

e) Proteins that have an antibody available are highlighted in grey.